

## On the Distribution of Surface Extrema in Several One- and Two-dimensional Random Landscapes

F. Hivert,<sup>1</sup> S. Nechaev,<sup>2,4</sup> G. Oshanin<sup>3,5</sup> and O. Vasilyev<sup>3,6</sup>

Received September 23, 2005; accepted October 9, 2006

Published Online: January 5, 2007

---

We study here a standard next-nearest-neighbor (NNN) model of ballistic growth on one- and two-dimensional substrates focusing our analysis on the probability distribution function  $P(M, L)$  of the number  $M$  of maximal points (i.e., local “peaks”) of growing surfaces. Our analysis is based on two central results: (i) the proof (presented here) of the fact that uniform one-dimensional ballistic growth process in the steady state can be mapped onto “rise-and-descent” sequences in the ensemble of random permutation matrices; and (ii) the fact, established in Ref. [G. Oshanin and R. Voituriiez, *J. Phys. A: Math. Gen.* **37**:6221 (2004)], that different characteristics of “rise-and-descent” patterns in random permutations can be interpreted in terms of a certain continuous-space Hammersley-type process. For one-dimensional system we compute  $P(M, L)$  exactly and also present explicit results for the correlation function characterizing the enveloping surface. For surfaces grown on 2d substrates, we pursue similar approach considering the ensemble of permutation matrices with long-ranged correlations. Determining exactly the first three cumulants of the corresponding distribution function, we define it in the scaling limit using an expansion in the Edgeworth series, and show that it converges to a Gaussian function as  $L \rightarrow \infty$ .

---

**KEY WORDS:** ballistic growth, distribution of extremal points, random permutation, Eulerian random walk

---

<sup>1</sup> LITIS/LIFAR, Université de Rouen, 76801 Saint Etienne du Rouvray, France.

<sup>2</sup> LPTMS, Université Paris Sud, 91405 Orsay Cedex, France.

<sup>3</sup> LPTMC, Université Paris 6, 4 Place Jussieu, 75252 Paris, France.

<sup>4</sup> P.N. Lebedev Physical Institute of the Russian Academy of Sciences, 119991 Moscow, Russia.

<sup>5</sup> Max-Planck-Institut für Metallforschung, Heisenbergstr. 3, D-70569 Stuttgart, Germany, and Institut für Theoretische und Angewandte Physik, Universität Stuttgart, Pfaffenwaldring 57, D-70569 Stuttgart, Germany.

<sup>6</sup> Center for Molecular Modelling, Materia Nova, University of Mons-Hainaut, Mons, Belgium.

## 1. INTRODUCTION

Within the recent years much effort has been devoted to theoretical analysis of properties of surfaces obtained by aggregation of particles. Several models describing various properties of clusters grown by different deposition processes have been proposed. To name but a few, we mention the famous Kardar–Parisi–Zhang (KPZ)<sup>(1)</sup> and the Edwards–Wilkinson (EW) models,<sup>(2)</sup> models of surfaces grown by Molecular Beam Epitaxy (MBE) (see, for example, Ref. 4), Polynuclear Growth (PNG)<sup>(5–8)</sup> and by Ballistic Deposition (BD),<sup>(10–13,19)</sup> in which case particles are sequentially added to a growing surface along ballistic trajectories with random initial positions and specified direction.

For these models of surface growth, a number of important theoretical achievements concerning the statistics of extrema has been made. In particular, in Ref. 3, the distributions of the maximal heights of the 1D Edwards–Wilkinson and of the KPZ interfaces were determined exactly. In Ref. 6, it was realized that the height distribution of the PNG surfaces coincides with the so-called Tracy–Widom distribution,<sup>(9)</sup> which appears in the theory of random matrices. In Refs. 14–16, it has been shown that in the thermodynamic limit BD exhibits the KPZ scaling behavior. Moreover, a discrete BD model has been shown recently to be a very convenient tool for studying non-Abelian entanglement properties of braided directed random walks.<sup>(18)</sup> Finally, it has been found that in many models of ballistic growth, as well as in their continuum-space counterparts belonging to the KPZ universality class,<sup>(1)</sup> the average velocity of cluster's growth is governed by the density of local minima of the enveloping surface.<sup>(19)</sup>

In these works the most attention was paid to the study of the statistics of local heights and corresponding scaling exponents of the enveloping surface. At the same time, the form of the distribution function of the density of local extrema (and of the corresponding moments of the distribution function) is much less investigated. The moments of the local maxima distribution depend on the microscopic details of the lattice model under consideration, and, hence, are less universal characteristics than, say, the roughness exponent. Nevertheless, the investigation of the distribution function is important for gaining deeper understanding of the morphological structure of a growing heap. For example, the expectation of the density of local maxima in the ballistically growing (1+1)D heap is  $1/3 = 0.333\dots$  (for  $L \gg 1$ , where  $L$  is the size of the surrounding box)—the precise definition of the model is given below. At the same time, the mean volume density of the (1+1)D heap is about 0.25 (for  $L \gg 1$ ). The last number is obtained in numerical experiment. Yet we have only the qualitative explanations of the difference between surface and volume densities of the heap and a deeper analysis of this question seems to us very important and rather intriguing from the physical point of view.

In our work we analyze the structure of the enveloping surface in a standard widely considered next-nearest-neighbor (NNN) model of ballistic growth<sup>(14,15,16)</sup> on one- and two-dimensional substrates. This model is known in the literature since many years and is recognized as a very convenient and simple lattice model which catches many basic properties of randomly growing substrates. Interpreting this model in terms of permutations of the set  $1, 2, 3, \dots, L$ , where  $L$  is the number of lattice sites and the numbers drawn at random from this set determine local heights of the surface, we calculate the Probability Distribution Function (PDF) of the number of maximal points (i.e., local “peaks”). Our analysis is based on two central results:

- (i) A proof, presented in this paper, of the fact that a ballistic growth process in the steady state can be formulated exactly in terms of a “rise-and-descent” pattern in the ensemble of random permutation matrices;
- (ii) An observation made in Ref. 24, that the “rise-and-descent” patterns can be treated efficiently using a recently proposed algorithm of a Permutation Generated Random Walk.

We remark that the expected value and the variance of the number of local peaks in surfaces grown by ballistic deposition on a one-dimensional and on a two-dimensional honeycomb lattices have been already calculated by J. Desbois in Ref. 20, using a certain decoupling of the hierarchy of coupled differential equations describing evolution of the moments of higher order. This method provides correct results for the first two moments of the distribution function and, apparently, may be extended further for the calculation of higher moments by truncation of the higher level correlations. However, this approach is not completely rigorous. Our approach, on contrary, is mathematically exact, does not rely on any uncontrollable assumption and enables us to go beyond the results obtained in Ref. 20. In particular, in one dimension we calculate a complete distribution function of the number of local peaks exactly. Apart of that, we also present explicit results for the correlation functions characterizing the enveloping surface. For surfaces emerging in two-dimensional ballistic growth, we reduce the problem to the analysis of the ensemble of permutation matrices with long-ranged correlations. Determining exactly the first three cumulants of the corresponding PDF, we obtain the distribution function in the scaling limit using expansions in the Edgeworth series.

The paper is outlined as follows. In Sec. 2 we formulate our models in one- and two-dimensions, discuss, on an intuitive level, a relation between a sequential growth of patterns in ballistic aggregation and “dynamics” on permutations, and finally present the main results of this work. Section 3 is devoted to a rigorous description of the relation between ballistic deposition and an “updating” dynamics on permutations. Further on, in Sec. 4 we analyze the probability distribution function of the number of local peaks on one-dimensional substrates. Here, we briefly outline the well-known results of Stembridge on the peak numbers,<sup>(21)</sup> describe the

model and basic results obtained for the so-called Permutation Generated Random Walks<sup>(24)</sup> and show how the operator formalism developed in this work can be extended for the calculation of the moments of the probability distribution function. Next, in Sec. 5 we present a derivation of an explicit expression of the probability of having two local surface peaks at distance  $l$  apart of each other (such that there is no peaks inbetween). In Sec. 6 we focus on two-dimensional situation and show how our previous analysis can be extended to this case. We calculate exactly first three cumulants of the corresponding probability distribution function of having  $M$  peaks on a square lattice containing  $L$  sites and then, using an expansion in the Edgeworth series, show that this function converges to a Gaussian as  $L \rightarrow \infty$ . Finally, in Sec. 7 we conclude with a brief summary of our results.

## 2. MODELS, DEFINITIONS AND MAIN RESULTS

### 2.1. Surfaces in Standard Ballistic Growth Process

A standard one-dimensional ballistic deposition model with next-nearest-neighboring (NNN) interactions is formulated as follows (for more details, see Refs. 14–16). Consider a box divided in  $L$  columns (of unit width each) enumerated by index  $i$  ( $i = 1, 2, \dots, L$ ). For simplicity, we assume the periodic boundary conditions, such that the leftmost and the rightmost columns are neighbors.

At the initial time moment, ( $n = 0$ ), the system is deemed empty. Then, at each tick of the clock,  $n = 1, 2, \dots, N$ , we deposit an elementary cell (“particle”) of unit height and width in a randomly chosen column. Suppose that the distribution on the set of columns is uniform. Define the height,  $h(i, n)$ , in the column  $i$  at time moment  $n$ . Assume now, as it is depicted in Fig. 1, that the cells in the nearest-neighboring columns interact in such a way that they can only touch each other by corners, but never by their vertical sides. This implies that after having deposited a particle to the column  $i$ , the height of this column is modified according to the following rule:

$$h(i, n + 1) = \max\{h(i - 1, n), h(i, n), h(i + 1, n)\} + 1. \quad (1)$$

If at the time moment  $n$  nothing is added to the column  $i$ , its height remains unchanged:  $h(i, n + 1) = h(i, n)$ . A set of deposited particles forms a pile as shown in Fig. 1a for  $L = 6$  columns and  $N = 6$  particles. Here, for example,  $h(1, 6) = 1$ ,  $h(2, 6) = 2$ , etc.

Now, we call the local maxima of the pile as the “peaks.” More specifically, take the set  $\mathcal{H}$  of heights at some time moment  $n$ :  $\mathcal{H} = \{h(1, n), h(2, n), \dots, h(L, n)\}$ . We say that the column  $i$  contains a “peak” at time moment

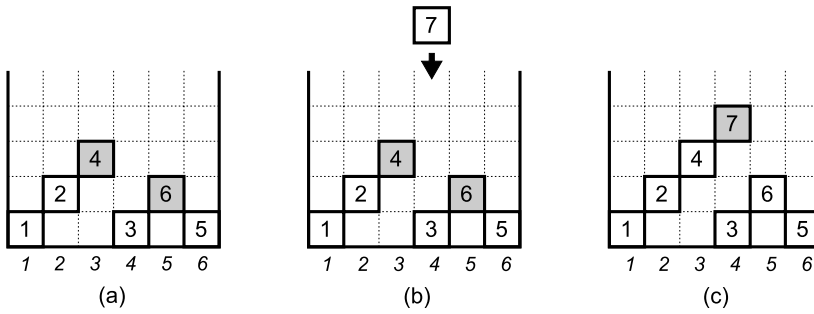


Fig. 1. Sequential growth of a heap in the ballistic deposition process.

$n$  if the height of this column satisfies the following two-sided inequality:

$$\begin{cases} h(i, n) > h(i - 1, n) \\ h(i, n) > h(i + 1, n). \end{cases} \quad (2)$$

Note that in Fig. 1a,b there are two peaks situated in the columns  $i = 3$  and  $i = 5$  and in Fig. 1c there is only one peak situated in the columns  $i = 4$ . The collection of peaks  $\mathcal{T}$  is the subset of  $\mathcal{H}$  and forms the “roof”—the set of upmost (or “removable”) particles. In Fig. 1 peaks are denoted by gray squares and other particles—by white ones. The relation of this ballistic deposition process with the “updating dynamics” on permutations is schematically depicted in Fig. 2. We briefly describe it below in Subsection B and in the Sec. 3 in more detail.

In a similar fashion, the process of a two-dimensional ballistic deposition in a box with a square base  $L = m \times m$ , ( $m$  is an integer), can be viewed as a sequential adding of elementary cubes in the columns satisfying the following rules (compare to (1)):

$$h(i, j, n + 1) = \max\{h(i - 1, j, n), h(i + 1, j, n), h(i, j, n), h(i, j - 1, n), h(i, j + 1, n)\} + 1, \quad (3)$$

where  $h(i, j, n)$  is the height of the column with coordinates  $(i, j)$  ( $1 \leq \{i, j\} \leq m$ ) at deposition moment  $n$  ( $1 \leq n \leq N$ ). The cubes are added to the columns with the uniform distribution—see Fig. 3.

The “peak” of a two-dimensional landscape  $h(i, j, n)$  is defined as a local maximum in the set  $\{h(i, j, n)\}$  for some fixed moment  $n$ , if the following

<sup>7</sup> Only the particle of the roof  $\mathcal{T}$  can be removed from the pile without disturbing the rest of the heap—as in the *mikado* game.

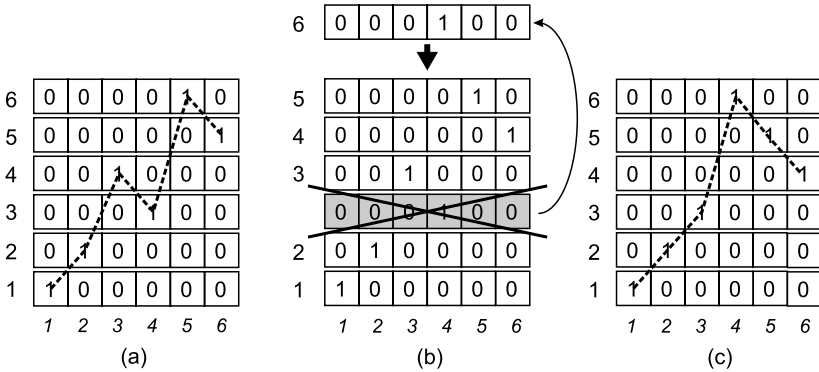


Fig. 2. An “updating dynamics” on permutations.

conditions are simultaneously fulfilled:

$$\begin{cases} h(i, j, n) > h(i - 1, j, n) \\ h(i, j, n) > h(i + 1, j, n) \\ h(i, j, n) > h(i, j - 1, n) \\ h(i, j, n) > h(i, j + 1, n) \end{cases} \quad (4)$$

Let us note that (3)–(4) assume periodic boundary conditions both in  $i$  and  $j$  coordinates ( $1 \leq \{i, j\} \leq m$ ). The influence of the boundary condition on the expectation, variance and higher moments of peak numbers can be easily estimated and becomes negligible in the limit  $m \rightarrow \infty$ .

For these models, our goal is to evaluate the probability distribution function  $P(M, L)$  of having  $M$  peaks on a lattice containing  $L$  sites. As we proceed to show, in one-dimension this can be done exactly. Moreover, we are also able to calculate the “correlation function”  $p(l)$  defining the conditional probability that two peaks are separated by the interval  $l$  under the condition that the interval  $l$  does not contain peaks. In 2d, determining exactly first three cumulants of the PDF we define it in the scaling limit using expansion in the Edgeworth series and show that it converges to a Gaussian function as  $L \rightarrow \infty$ .

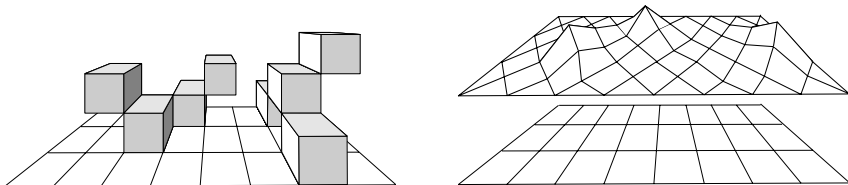


Fig. 3. Two-dimensional ballistic deposition and corresponding random landscape.

**2.2. Interpretation of Ballistic Growth: “Updating Dynamics” and Random Permutations of Natural Series**

Let us emphasize that we are interested only in the statistics of peaks of a growing surface in the *stationary state* and disregard any questions concerning the statistics of heights.

Dynamics of the set of peaks  $\mathcal{T}$  in the ballistic deposition process depicted in Fig. 1 can be mapped onto the dynamics of “peaks” in the permutation matrix. We start by describing this connection on an intuitive level. To do this, let us proceed recursively. Suppose that we deposit a first particle in the column  $i_1$  of an  $L$ -column box. Next, take the row of  $L$  elements with “1” at position  $i_1$  and

“0” in all other places:  $(\overbrace{0, \dots, 0}^{i_1-1}, 1, 0, \dots, 0)$ . After dropping the second particle,

say, in the column  $i_2$ , take a row  $(\overbrace{0, \dots, 0}^{i_2-1}, 1, 0, \dots, 0)$  and place it over the first one creating a stack. Suppose that at some time  $n$  a new particle is added to the column which was occupied earlier, say, at time  $m$ , i.e.  $i_n = i_m$  ( $n > m$ ). It means that we have two identical rows in the stack. In this case, we remove the first of identical rows (i.e. deposited at time  $m$ ) from the stack and eliminate the empty line by pulling down all rows deposited after time  $m$ , as it is depicted in Fig. 2d. After some time, the stack will comprise  $L$  rows and, according to the described procedure, will not grow anymore but will be changed only due to updating of rows (by adding the new ones and by eliminating the old ones). By construction, this stack is an  $L \times L$  permutation matrix. Connecting the nonzero elements in nearest-neighboring rows by a broken line, we can straightforwardly define the “descents,” “rises” and “peaks” in the permutation matrix—see Fig. 2c. The number of peaks at time  $N$  in the  $L \times L$  permutation matrix coincides then with the number of peaks in the heap after having deposited  $N$  particles in a box of  $L$  columns. The rigorous proof of this mapping is given in the Sec. 3.

Consequently, the described relation between the original ballistic deposition model and an “updating” dynamics on permutations, depicted in Fig. 2c,d, allows us to view the characteristics of the surface obtained within the BD process from a different perspective: Consider, for example, a one-dimensional lattice containing  $L$  sites, on which we distribute numbers drawn randomly from the set  $1, 2, 3, \dots, L$ . A number appearing at the site  $j$  determines the local “height”<sup>8</sup> of the surface. Now, we call this site as “a peak,” if the number appearing on this site is bigger than the numbers on two neighboring sites—see Fig. 4. Generalization to two-dimensional square lattice with  $L = m \times m$ , ( $m$  is

<sup>8</sup>Note that the “heights” appearing in permutation matrices have nothing to do with real heights in the original BD growth model.

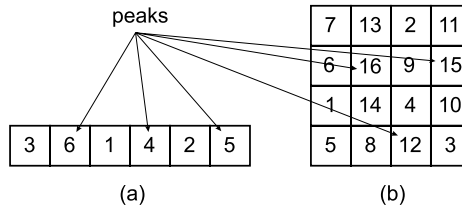


**Fig. 4.** (a) One-dimensional ( $L = 6$ ) and (b) two-dimensional square ( $L = 4 \times 4$ ) lattices with periodic boundary conditions on sites of which we distribute numbers drawn from the set  $1, 2, 3, \dots, L$ . These numbers determine the local heights of the surface. The sites with numbers bigger than those appearing on the neighboring sites are referred to as the “peaks.”

an integer) sites is straightforward—see Fig. 4b: the only difference here is that we call as local “surface peaks” such sites  $j$  the numbers at which are bigger than numbers appearing at four adjacent sites. We prove rigorously in what follows that the probability of having  $M$  peaks on a lattice containing  $L$  sites on which we place numbers randomly drawn from the set  $1, 2, 3, \dots, L$ , and the distribution function  $P(M, L)$  characterizing the number of local surface maxima in the surfaces of aggregates grown within the BD process, are *identic*. We note finally that the peak statistics in the latter model with natural numbers  $1, 2, 3, \dots, L$  and in a related model with a lattice on sites of which one places randomly numbers uniformly distributed in  $[0,1]$  has very interesting and unexpected features, as was recently communicated to us by B. Derrida.<sup>(17)</sup>

### 2.3. Main Results

Main results of this work are as follows:

- (i) We prove that a uniform one-dimensional ballistic growth process in the steady state can be mapped onto the “rise-and-descent” sequences in the ensemble of random permutation matrices.
- (ii) We show that in one dimension the probability distribution function  $P(M, L)$  can be calculated exactly through its generating function

$$W(s, L) = L! \sum_{M=0}^{\infty} s^{M+1} P(M, L), \tag{5}$$

where

$$W(s, L) = \left( \frac{s}{1 - \sqrt{1-s}} \right)^{L+1} \sum_{M=0}^{\infty} \left( \frac{(1 - \sqrt{1-s})^2}{s} \right)^{M+1} A(M, L) \tag{6}$$

with  $A(M, L)$  being the so-called Eulerian numbers counting the number of “rises” (or “descents”) in the ensemble of equally weighted permutation



matrices of size  $L$ :

$$A(M, L) = \sum_{r=0}^M (-1)^r \binom{L+1}{r} (M-r)^L, \tag{7}$$

where  $\binom{a}{b}$  denotes the binomial coefficient; here and henceforth we adopt a standard notation when  $\binom{a}{b} = \frac{a!}{b!(a-b)!}$  for  $0 \leq b \leq a$  and  $\binom{a}{b} \equiv 0$  otherwise.

Inverting (5), we find the following exact expression for  $P(M, L)$ :

$$P(M, L) = \frac{2^{L+2}}{L!} \sum_{l=1}^M (-1)^{M-l} \binom{\frac{L+1}{2}}{M-l} \sum_{m=1}^l \frac{m^{L+1}}{(l-m)!(l+m)!} \tag{8}$$

In the limit  $L \rightarrow \infty$ , the PDF  $P(M, L)$  converges to a Gaussian distribution:

$$P(M, L) \sim \frac{3}{2} \sqrt{\frac{5}{\pi L}} \exp \left\{ -\frac{45(M - \frac{1}{3}L)^2}{4L} \right\}. \tag{9}$$

Note that a similar result has been previously found in Ref. 24 for the sum of peaks and troughs in a permutation of length  $L$  within the context of the number of the U-turns made by the ‘‘Permutation Generated Random Walk’’ (PGRW).

- (iii) We show that in one-dimensional systems the probability  $p(l)$  of having two peaks separated by the interval  $l$  under the condition that this interval does not contain other peaks, obeys:

$$p(l) = 2^l \frac{(l-1)(l+2)}{(l+3)!}$$

Curiously enough, this expression coincides with the distribution function of the distance between two ‘‘weak’’ bonds obtained by Derrida and Gardner <sup>(27)</sup> in their analysis of the number of metastable states in a one-dimensional random Ising spin glass at zero’s temperature.

- (iv) Using the cumulant expansion, we show that in two dimensions, in the limit  $L \rightarrow \infty$ , the normalized probability distribution function  $p(x, L)$ , where  $x = (M - \mu_1^{2D})/\sigma$ , converges to a Gaussian distribution

$$p \left( x = \frac{M - \mu_1^{2D}}{\sigma}, L \right) \rightarrow \frac{1}{\sqrt{2\pi}} e^{-x^2/2} \left( 1 + \frac{1}{\sqrt{L}} f(x) + o \left( \frac{1}{\sqrt{L}} \right) \right),$$

where

$$f(x) = \sqrt{L} \frac{\kappa_3^{2D}}{(\kappa_2^{2D})^{3/2}} \frac{1}{6} (x^3 - 3x)$$

where the cumulants,  $\kappa_i^{2D}$ , coincide with the central moments,  $\mu_i^{2D}$ , ( $i = 1, 2, 3$ ). The last ones are as follows:

$$\begin{cases} \mu_1^{2D} = \frac{1}{5}L \\ \mu_2^{2D} = \sigma^2 = \frac{13}{225}L \\ \mu_3^{2D} = \frac{512}{32175}L \end{cases}$$

- (v) We have realized that local peaks in one-and two-dimensional equilibrium NNN ballistic deposition model are correlated and the correlation length extends over two lattice spacings: while by definition, the probability of having two peaks at the neighboring sites is zero, appearance of two peaks on next-nearest-neighboring sites (also on a diagonal for 2d) is higher than squared mean density of peaks ( $1/9$  and  $1/25$  in 1d and 2d, respectively). On contrary, the probability of having two peaks at a distance exceeding two lattice spacings is equal to the squared mean density, which signifies that they are uncorrelated. In other words, there are effective short-range “attractive” interactions between peaks. The corresponding weights of a few typical configurations are summarized in Fig. 5.

### 3. RIGOROUS DESCRIPTION OF THE RELATION BETWEEN “UPDATING DYNAMICS” ON PERMUTATIONS AND BD

As we have already mentioned in the previous section, dynamics of the set of peaks  $\mathcal{T}$  in the ballistic deposition process depicted in Fig. 2 can be mapped onto the dynamics of “peaks” in the permutation matrix. Let us formulate this mapping explicitly.

In a more rigorous approach, we have to consider two dynamical systems: one—on peak sets and the other—on permutations. Let us call  $E_i$  the operation which corresponds to dropping a box in the column  $i$  on a peak set. That is if  $S$  is a peak set (i.e. a subset of  $\{1, \dots, L\}$  without two consecutive numbers) then

$$E_i(S) := S \cup \{i\} / \{i-1, i+1\}. \quad (10)$$

The corresponding operation  $F_i$  on permutations is defined by

$$\mu := F_i(\sigma) \quad \text{with} \quad \mu(k) := \begin{cases} \sigma(k) & \text{if } \sigma(k) < \sigma(i) \\ L & \text{if } k = i \\ \sigma(k) - 1 & \text{if } \sigma(k) > \sigma(i) \end{cases} \quad (11)$$

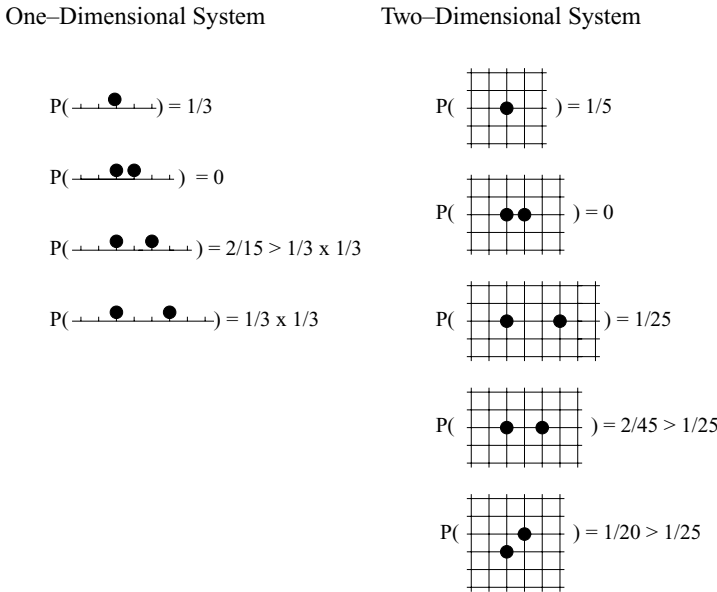


Fig. 5. Probabilities of having a single peak and a pair of isolated peaks some distance apart from each other in one and two-dimensional models. Filled circles denote peaks—sites with numbers exceeding numbers appearing on nearest-neighboring sites. First column presents probabilities of several configurations in 1d, while the second one describes the probabilities of a few possible configurations appearing in two dimensions.

To proceed, we also need to define the reverse operation on permutations,  $R_k$ , which removes the upmost row and inserts it under the row  $k$ :

$$\mu := R_k(\sigma) \quad \text{with} \quad \mu(l) := \begin{cases} \sigma(l) & \text{if } \sigma(l) < k \\ k & \text{if } \sigma(l) = L \\ \sigma(l) + 1 & \text{if } L > \sigma(l) > k \end{cases} \quad (12)$$

It is clear now that  $F_i(\sigma) = \mu$  if and only if  $R_k(\mu) = \sigma$  where  $k = \sigma(i)$  is the row of the 1 in the column  $i$ .

Denote now by  $\text{Peak}(\sigma)$  the peak set of the permutation  $\sigma$ . Then, it is obvious that for all permutation  $\sigma$

$$E_i(\text{Peak}(\sigma)) = \text{Peak}(F_i(\sigma)) \quad \text{for all } i \leq L. \quad (13)$$

This simple but crucial observation allows us to translate the dynamics on permutations to the dynamics of peak sets. We will proceed in two steps: first, we will show that the limit probability measure of the dynamical system on permutations is equi-distributed and second, we will demonstrate that the image of this

probability measure by the peak-set map is the limit probability measure on peak sets.

Let  $(P(\sigma))_\sigma$  be a probability measure on permutations. Then, after one uniformly random chosen step  $F_i$  the new probability  $P'(\mu)$  of a permutation  $\mu$  is

$$P'(\mu) = \frac{1}{L} \sum_{i=1}^L \sum_{\sigma} P(\sigma) \tag{14}$$

where the inner sum extends over the sets of all permutations  $\sigma$ , such that  $F_i(\sigma) = \mu$ . However, by definition of  $F_i$ , if a permutation  $\tau$  is of the form  $\tau = F_i(\sigma)$  then  $\tau(i) = L$ . Thus in the previous sum the only value of  $i$  such that there exists some  $\sigma$  such that  $F_i(\sigma) = \mu$  is  $i = \mu^{-1}(L)$ , that is if  $i$  is the column where the 1 is in the top row  $L$  in  $\mu$ . Now, here are exactly  $L$  permutations  $\sigma$  verifying  $F_i(\sigma) = \mu$ , namely  $R_k(\mu)$  for  $k = 1 \dots L$ . Consequently,  $P'(\mu)$  is simply the average of the probabilities of the  $R_k(\mu)$ :

$$P'(\mu) = \frac{1}{L} \sum_{k=1}^L P(R_k(\mu)). \tag{15}$$

Moreover, it is clear that for all pairs of permutations  $\sigma, \mu$  there is a sequence  $(i_r)_r$  of transformations which maps  $\sigma$  on  $\mu$ , that is  $\mu = \dots F_{i_3} F_{i_2} F_{i_1}(\sigma)$ . Consequently, the map  $F : P \mapsto P'$  is an irreducible Perron-Frobenius map whose maximal module eigenvalue is 1 with multiplicity 1. Thus, when the number of boxes tends to infinity, the probability converges to some limit and this limit is the unique, normalized (the sum of the coordinate is 1) eigenvector of  $F$  corresponding to the eigenvalue 1. In virtue of (15), the uniform distribution on permutations is preserved by  $F$  so that it must be the limit distribution.

Using (13), it is possible to translate our permutations language to the language of the peak sets. Recall that we call a peak set any subset of  $\{1, \dots, L\}$  without two consecutive numbers. The only needed remark is that any non empty peak set  $S$  is the peak set of a permutation. Thus the map Peak extends to a surjective map from the set of probability measure on permutations to the set of probability measures on peak sets:

$$\text{Peak} : P \longmapsto \text{Peak}(P)(S) := \sum_{\sigma : \text{Peak}(\sigma)=S} P(\sigma). \tag{16}$$

Denote next  $E$  the map  $P(S) \mapsto P'(S)$  where  $P'(S)$  is the new probability measure on sets after a uniformly random step  $E_i$ . Then (13) can be written down as

$$E(\text{Peak}(P)) = \text{Peak}(F(P)), \tag{17}$$

for all probability measures on permutations  $P$ . In particular, the spectrum of  $E$  is included in the spectrum of  $F$  and moreover, the generalized eigenspaces (kernel

of  $(F - \lambda I)^m$  for  $m$  large) of  $E$  are the image under Peak of the generalized eigenspaces of  $F$ . Consequently,  $E$  is a Perron-Frobenius map with maximal module eigenvalue 1 with multiplicity 1. As a consequence the limit distribution on peak sets exists and is the image by the map Peak of the limit distribution on permutations

$$P_{\text{limit}}(S) = \text{Peak}(P_{\text{limit}}(\sigma))(S) = \frac{1}{L!} \#\{\sigma \mid \text{Peak}(\sigma) = S\}. \tag{18}$$

Before we proceed further, a few comments might be in order:

First, as a matter of fact, this technique is quite general and can be applied to a more general notion of heaps of pieces. We demonstrate it on the following example. Let  $G = (V, E)$  be a finite oriented simple graph with vertex and edge set  $V$  and  $E$  and let  $L$  be the number of vertices. Each vertex  $v \in V$  is associated with one “type” of pieces, and an arrow  $e = v \mapsto v'$  encodes the fact that when a piece of type  $v$  falls after a piece of type  $v'$ , then it is placed over it, thus they are no more pieces of type  $v'$  at the top of the pile. The notion of permutation generalizes to the notion of standard labelling of the vertex of the graph, that is assignation of distinct numbers from  $1 \dots L$  to the vertices  $v$ . Then a vertex  $v$  is called a peak of a labelling  $l$  if  $l(v) > l(v')$  for all edges  $v \mapsto v'$ . One immediately notices that the previous reasoning applies, which implies that for all sets  $S$  of vertices the limit probability measure  $P_{\text{limit}}(S)$  of  $S$  to be exactly the set of maximal pieces of a random heaps on the graph  $G$  is given by (18). In this regard, the limit distribution of the 2D models can also be computed using these generalized peaks. Moreover, in the case of the oriented lines the notion of peaks reduces to the notion of a descents.

Second, combinatorics of peaks of permutations has been recently reviewed by J. Stembridge in Ref. 21. The peak algebra of Stembridge is a certain sub-algebra of the algebra of polynomials with infinitely many variables. It has a natural basis  $K_S$  indexed by peak sets  $S$  and therefore can serve as the support for generating series of probability of a peak set. In this regard, the generating series of the probability of each peak set has a very simple expression

$$\sum_{L=0}^{\infty} t^L \sum_{S \subset \{1 \dots L\}} P(S) K_S = \sum_{L=0}^{\infty} \frac{t^L}{L!} \sum_{S \subset \{1 \dots L\}} \#\{\sigma \mid \text{Peak}(\sigma) = S\} K_S = \exp(K_1 t) \tag{19}$$

where  $K_1$  is the unique peak set where  $L = 1$ . Note that there is a minor difference between our work and Ref. 21, since in the latter the extremities 1 and  $L$  were never considered as a peak, while we use the periodic boundary conditions. This difference should be unimportant for sufficiently large  $L$ .

Furthermore it should be noticed that in Ref. 23, a different random walk is considered on peaks and conjectured on permutations with the same limit probability measure. Finally, the result of Ref. 22, suggests that this

measure should be seen as some kind of generalized Plancherel measure associated with the degenerated Hecke-Clifford algebra instead of the symmetric group.

#### 4. PROBABILITY DISTRIBUTION FUNCTION $P(M, L)$ IN 1D

We are now in position to determine exactly the probability  $P(M, L)$  that a random heap has a fixed number of peaks. From our previous analysis, it follows that such a probability is equal to the number  $B(M, L)$  of permutations of length  $L$  having exactly  $M$  peaks, divided by the total number of permutations  $L!$ , i.e.  $P(M, L) = B(M, L)/L!$ . Now, we recollect that if one considers permutation descents instead of peaks, the numbers  $A(M, L)$  of permutations of  $1 \dots L$  with exactly  $M$  descents are known as the Eulerian numbers, obey the following three-site recursion

$$A(M, L) = (L - M + 1) A(M - 1, L - 1) + M A(M, L - 1) \quad (20)$$

which leads to the following recurrence relation for the generating function  $U(t, L) = \sum_{M=0}^{\infty} t^{M+1} A(M, L)$ :

$$U(t, 1) = t, \quad U(t, L) = t(1 - t) \frac{d}{dt} U(t, L - 1) + LtU(t, L - 1). \quad (21)$$

The recursion relation for peak-Eulerian number  $B(M, L)$  has been considered by Stembridge in Ref. 21, Remark 4.8. In our notations, his results attains the following form

$$B(M, L) = (L - 2M + 2) B(M - 1, L - 1) + 2M B(M, L - 1) \quad (22)$$

which in turn can be encoded by the recurrence relation obeyed by the generating series  $W(s, L) = \sum_{M=0}^{\infty} s^{M+1} B(M, L)$  (note that compared to Stembridge there is no  $s^{k+1}$  term):

$$W(s, 1) = s, \quad W(s, L) = 2s(1 - s) \frac{d}{ds} W(s, L - 1) + LsW(s, L - 1). \quad (23)$$

Here is a table of a few first polynomials  $W(s, L)$ :

$$\begin{aligned}
 W(s, 1) &= s \\
 W(s, 2) &= 2s \\
 W(s, 3) &= 2s^2 + 4s \\
 W(s, 4) &= 16s^2 + 8s \\
 W(s, 5) &= 16s^3 + 88s^2 + 16s \\
 W(s, 6) &= 272s^3 + 416s^2 + 32s \\
 W(s, 7) &= 272s^4 + 2880s^3 + 1824s^2 + 64s \\
 W(s, 8) &= 7936s^4 + 24576s^3 + 7680s^2 + 128s \\
 W(s, 9) &= 7936s^5 + 137216s^4 + 185856s^3 + 31616s^2 + 256s
 \end{aligned}
 \tag{24}$$

Differentiating polynomials  $W(s, L)$  and setting  $s = 1$ , we can find, in principle, any moments of the probability distribution function. For example, the expectation of the number of peaks is  $\frac{L+1}{3}$  for  $L \geq 2$ ; the variance is  $\frac{2L+2}{45}$  for  $L \geq 4$ , while the third central moment is equal to  $-\frac{2L+2}{945}$  for  $L \geq 8$ .

### 4.1. Permutation Generated Random Walks

In this subsection we briefly outline the basic notions concerning the so-called Permutation Generated Random Walk (PGRW) proposed in Ref. 24. Consider a given permutation  $\pi = \{\pi_1, \pi_2, \pi_3, \dots, \pi_{L+1}\}$  of  $[L + 1] = 1, 2, 3, \dots, L + 1$  and rewrite it as a 2-line table:

$$\pi = \begin{pmatrix} 1 & 2 & 3 & \dots & L + 1 \\ \pi_1 & \pi_2 & \pi_3 & \dots & \pi_{L+1} \end{pmatrix}.$$

Suppose that this table assigns some discrete “time” variable  $j$  ( $j = 1, 2, 3, \dots, L + 1$ , upper line in the table) to each permutation encountered in the second line and, hence, allows to order this permutation.

Now, in a standard notation, we call  $j$  the “rise,” if  $\pi_j < \pi_{j+1}$ , otherwise, if  $\pi_j > \pi_{j+1}$ , we refer to it as the “descent.” Further on, if we have simultaneously  $\pi_{j-1} < \pi_j$  and  $\pi_j > \pi_{j+1}$ , we call  $j$  - the “peak.”

Then, the Permutation Generated Random Walk is defined by the following recursive procedure:

- (i) at time moment  $j = 0$  the walker is at the origin;
- (ii) at time  $j > 0$  the walker makes a step to the right if  $j$  is the rise, and makes a step to the left if  $j$  is the descent.

Note that, evidently, if  $j$  is a peak, the walker makes a left “U-turn.”

Statistical properties of the PGRW were studied in Ref. 24, where the distribution of the end-to-end distance and intermediate points of the trajectory, probability measure of different trajectories, the number of U-turns, as well as various correlation functions have been analyzed with respect to the uniform measure on the ensemble of random permutations.

Using the methods developed in Ref. 24, and exploiting the connection between the one-dimensional ballistic deposition process and dynamics on permutations established in the previous section, one can straightforwardly reconstruct the probability distribution  $P(M, L)$  of having  $M$  peaks in the uniform ballistic deposition process in the planar box composed of  $L$  columns in the stationary regime. According to Ref. 21, the generating function of number of peaks  $W(s, L)$  can be expressed in terms of the generating function of the number of rises,  $U(t, L)$ , in the ensemble of equally weighted permutation matrices of size  $L$  (the so-called Eulerian number), Eq. (7). The explicit relation between  $W(s, L)$  and  $U(t, L)$  is:

$$W(s, L) = \left( \frac{2}{1+t} \right)^{L+1} U(t, L) \quad (25)$$

where

$$s = \frac{4t}{(1+t)^2}; \quad t = \frac{2-s-2\sqrt{1-s}}{s} = \frac{(1-\sqrt{1-s})^2}{s} \quad (26)$$

Taking into account the identity established in Ref. 24:

$$A(M, L) = \frac{2L!}{\pi} \int_0^\infty \left( \frac{\sin x}{x} \right)^{L+1} \cos(x(2M - L - 1)), \quad (27)$$

we arrive at the following explicit expression for the generating function  $W(s, L)$ :

$$\begin{aligned} W(s, L) &= \left( \frac{2}{1+t} \right)^{L+1} \sum_{M=0}^{\infty} t^{M+1} A(M, L) \\ &= \frac{2^{L+1} L!}{\pi (1+t)^{L+1}} \int_0^\infty dx \left( \frac{\sin x}{x} \right)^{L+1} \\ &\quad \times \frac{e^{-ix(L+1)} t \left( (1 + e^{2ix(3+L)}) t - e^{2ix(2+L)} - e^{2ix} \right)}{(1 + e^{4ix}) t - e^{2ix} (1 + t^2)} \end{aligned} \quad (28)$$

with  $t$  given by (26). Polynomials  $W(s, L)$  admit also another useful representation directly following from the relations between generating functions  $W(s, L)$  and



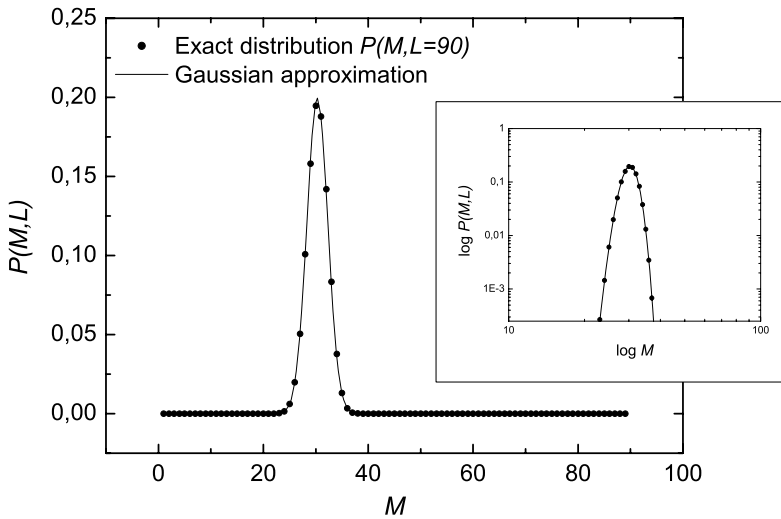


Fig. 6. Exact distribution function (8) (●) and its Gaussian approximation (9) (line) for  $L = 90$ . For better resolution the same results are shown in the insert in log-log scale.

$U(t, L)$  found in Ref. 21:

$$W(s, L) = 2^{L+2}(1 - s)^{(L+1)/2} \text{Li}_{-(L+1)}\left(\frac{(1 - \sqrt{1 - s})^2}{s}\right) \tag{29}$$

where  $\text{Li}_\nu(x)$  is the Poly-log function.

Exact expression for the distribution function  $P(M, L)$  obtained from (29) is given by Eq. (8). More details on its derivation are presented in the appendix. In the asymptotic limit  $L \gg 1$  the double sum (8) converges to a Gaussian function with a nonzero mean (9)—see Fig. 6.

Calculating the first three central moments of the limiting distribution function in Gaussian approximation (9) for  $L \gg 1$ , we get:

$$\begin{cases} \mu_1^{1D} = \sum_{M=1}^L M P(M, L) = \frac{1}{3}L, \\ \mu_2^{1D} = \langle (M - \langle M \rangle)^2 \rangle = \frac{2}{45}L, \\ \mu_3^{1D} = \langle (M - \langle M \rangle)^3 \rangle = 0. \end{cases} \tag{30}$$

Note that the first two expressions coincide with the expectation and the variance computed by J. Desbois in Ref. 20, using decoupling of the hierarchy of correlation functions. The third central moment, i.e.  $\mu_3^{1D}$ , of the distribution

$P(M, L)$ , naturally turns to be equal to 0 since the Gaussian limit is considered. In what follows we proceed to show using the method of the correlation functions (see the next Section for details) that all moments of the distribution may be calculated exactly, for arbitrary finite  $L$ . As a matter of fact, the value of  $\mu_3^{\text{1D}}$  is

$$\mu_3^{\text{1D}} = \langle (M - \langle M \rangle)^3 \rangle = -\frac{2}{945}L, \quad (31)$$

i.e. it is not zero and grows linearly with the system size  $L$  due to large deviations which are not taken into account in the Gaussian approximation. The value of  $\mu_3^{\text{1D}}$  coincides with the one computed using the generating function in (24) or (28).

#### 4.2. Correlation Functions of the PGRW within the Operator Formalism

In Ref. 24, it has been shown that a non-Markovian PGRW can be effectively described using an auxiliary, recursively constructed Markovian process, which has the same distribution as the PGRW. Employing the ideas of Hammersley<sup>(28)</sup> (see also Ref. 29, for more details), who has used such an approach in his celebrated analysis of the problem of the longest increasing subsequence in random permutations, the following random walk model has been constructed:

- Suppose one has an infinite in both directions line of integers and a random walker initially at the origin;
- Trajectory  $Y_l$  of this auxiliary process is built step by step: at time moment  $l$  define a real-valued random variable  $x_{l+1}$ , having a uniform distribution in  $[0, 1]$ . If  $x_{l+1} > x_l$  the walker is moved to the right, i.e.  $Y_l = Y_{l-1} + 1$ ; otherwise, it goes to the left, i.e.  $Y_l = Y_{l-1} - 1$ . At the next time moment, chose  $x_{l+2}$ , compare it with  $x_{l+1}$  and move the walker accordingly, and etc.

Two strong results have been proven in Ref. 24, concerning the relation between this recursively constructed Markovian process and the PGRW: First of all, it has been shown that the probability  $P(Y_L = X)$  for the trajectory  $Y_L$  of the auxiliary process to appear at site  $X$  at time moment  $L$  is equal to the probability  $P(X_L^{(L)} = X)$  for the end-point  $X_L^{(L)}$  of the PGRW trajectory  $X_l^{(L)}$  generated by a given permutation of  $[L + 1]$  to appear at site  $X$ . This signifies that

$$P(Y_L = X) = \frac{(1 - (-1)^{X+L})}{2L!} A\left(\frac{X + L - 1}{2}, L\right). \quad (32)$$

(Recall that  $A(\dots)$  is the Eulerian number).

Second, it has been proven that the probability  $P(X_l^{(L)} = X)$  for the PGRW trajectory  $X_l^{(L)}$  at intermediate time moment  $l = 1, 2, 3, \dots, L$  to appear at site  $X$

is equal to the probability  $P(Y_l = X)$  for the trajectory of the auxiliary process  $Y_l$  to appear at time moment  $l$  at site  $X$ . That is,

$$\begin{aligned}
 P(X_l^{(L)} = X) &= P(Y_l = X) = P(X_l^{(l)} = X) \\
 &= \frac{(1 - (-1)^{X+l})}{2l!} A\left(\frac{X+l-1}{2}, l\right),
 \end{aligned}
 \tag{33}$$

which signifies that distribution of any intermediate point  $X_l^{(L)}$  of the PGRW trajectory generated by permutations of a sequence of length  $L + 1$  depends on  $l$  but is independent of  $L$ .

Using this equivalence, it is thus possible to write down explicitly the probability measure of any given PGRW trajectory (or of some part of it) as a chain of iterated integrals over real-valued random variables  $x_l$ . Recollecting the definition of the PGRW and noticing that each trajectory mirrors one-by-one a unique “rise-and-descent” sequence in a random permutation, we are thus able to represent a probability of any “rise-and-descent” sequence as a chain of iterated integrals over real-valued random variables  $x_l$  uniformly distributed in  $[0, 1]$ .

More specifically, following Ref. 24, consider a given “rise-and-descent” sequence  $\alpha(L)$  of length  $L$  of the form:

$$\alpha(L) = \begin{pmatrix} 1 & 2 & 3 & \dots & L \\ a_1 & a_2 & a_3 & \dots & a_L \end{pmatrix}.$$

where  $a_l$  can take either of two symbolic values:  $\uparrow$  or  $\downarrow$ . Consequently, the first line in the table is the running index  $l$  which indicates position along the permutation, while the second line shows what we have at this position—a rise or a descent. Assign next to each symbol at position  $l$  an integral operator; for a rise ( $\uparrow$ ) it is  $I_l(\uparrow)$ , while for a descent ( $\downarrow$ ) it will be  $I_l(\downarrow)$ , where

$$\hat{I}_l(\uparrow) = \int_{x_{l-1}}^1 dx_l \quad \text{and} \quad \hat{I}_l(\downarrow) = \int_0^{x_{l-1}} dx_l.
 \tag{34}$$

To each  $L$ -step trajectory one associates next a characteristic polynomial  $Q(x, \alpha(L))$  defined as an “ordered” product:<sup>(24)</sup>

$$Q(x, \alpha(L)) = \prod_{l=1}^L \hat{I}_l(a_l) \cdot 1,
 \tag{35}$$

where  $a_l = \{\uparrow, \downarrow\}$  for  $l = 1, \dots, L$ . The statistical weight, i.e. the probability distribution function,  $P(\alpha(L))$ , of this given “rise-and-descent” sequence  $\alpha(L)$  in the ensemble of all equally likely permutations is then simply given by

$$P(\alpha(L)) = \int_0^1 Q(x, \alpha(L)) dx.
 \tag{36}$$

It may be expedient to illustrate this formal representation on a particular example. Consider, e.g., a given “rise-and-descent” sequence of the form  $\{\uparrow, \uparrow, \downarrow, \uparrow, \uparrow\}$ . For this sequence, the characteristic polynomial  $Q(x, \alpha(5))$  reads:

$$\begin{aligned} Q(x, \alpha(5)) &= \hat{I}_1(\uparrow) \hat{I}_2(\uparrow) \hat{I}_3(\downarrow) \hat{I}_4(\uparrow) \hat{I}_5(\uparrow) \cdot 1 \\ &= \int_x^1 dx_1 \int_{x_1}^1 dx_2 \int_0^{x_2} dx_3 \int_{x_3}^1 dx_4 \int_{x_4}^1 dx_5 \cdot 1 \\ &= \frac{3}{40} - \frac{x}{8} + \frac{x^3}{12} - \frac{x^4}{24} + \frac{x^5}{120}, \end{aligned}$$

and, hence, the probability of this particular configuration is

$$P(\alpha(5)) = \int_0^1 Q(x, \alpha(5)) dx = \frac{19}{720}.$$

We note that construction of the probability measure in (34)–(36) can be most easily understood by considering the following example. Suppose there are three “markers” representing the particles with the coordinates  $x_1, x_2, x_3$  ( $0 \leq \{x_1, x_2, x_3\} \leq 1$ )—see Fig. 7. Markers in Fig. 7 can be independently deposited in the interval  $[0, 1]$  with uniform distribution. It is obvious that the probability  $P(\uparrow \downarrow)$  for three particles to create a peak, is defined by the probability of a configuration with  $0 \leq x_1 < x_2$  and  $x_2 > x_3 \leq 1$ . Thus,

$$P(\uparrow \downarrow) = \int_0^1 dx_3 \int_{x_3}^1 dx_2 \int_0^{x_2} dx_1 \cdot 1 = \frac{1}{3},$$

what coincides with the operator expression

$$P(\uparrow \downarrow) = \int_0^1 \hat{I}_1(\uparrow) \hat{I}_2(\downarrow) dx.$$

(compare to (34)–(35)).

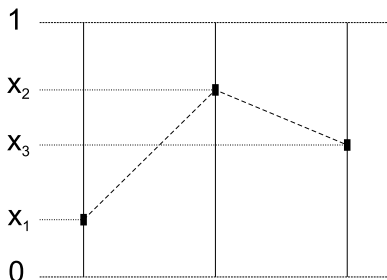


Fig. 7. Three markers creating a peak configuration.

### 4.3. Exact Calculation of the First Three Central Moments of the Distribution $P(M, L)$ in 1d

Now we apply the operator formalism for the computation of three first central moments of the probability distribution function,  $P(M, L)$ , of having  $M$  peaks on a one-dimensional periodic lattice of size  $L$ :

$$\begin{aligned} \mu_1^{1D} &\equiv \langle M \rangle, \\ \mu_2^{1D} &\equiv \langle M^2 \rangle - \langle M \rangle^2, \\ \mu_3^{1D} &\equiv \langle M^3 \rangle - 3\langle M \rangle \langle M^2 \rangle + 2\langle M \rangle^3. \end{aligned} \tag{37}$$

Let us introduce

$$\Delta_i^- = \theta(x_i - x_{i-1}) \quad \text{and} \quad \Delta_i^+ = \theta(x_i - x_{i+1}), \tag{38}$$

for  $i = 1, \dots, L$ , where  $\theta(x)$  is the Heaviside step-function

$$\theta(x) = \begin{cases} 1 & \text{for } x > 0, \\ 0 & \text{for } x \leq 0. \end{cases}$$

Because of the periodic boundary conditions we have  $\Delta_1^- = \theta(x_1 - x_L)$  and  $\Delta_L^+ = \theta(x_L - x_1)$ . Using the operator formalism we can represent the expectation  $\mu_1^{1D}$  in the following form

$$\mu_1^{1D} = \int_0^1 \int_0^1 \dots \int_0^1 \left[ \sum_{i=1}^L \Delta_i^- \Delta_i^+ \right] dx_1 dx_2 \dots dx_L. \tag{39}$$

In the sum above each term  $\Delta_i^- \Delta_i^+ = \theta(x_i - x_{i-1})\theta(x_i - x_{i+1})$  corresponds to the peak at the position  $x_i$ . All  $L$  terms in the sum in (39) are identical and independent, so it is possible to rewrite (39) as

$$\begin{aligned} \mu_1^{1D} &= L \int_0^1 \int_0^1 \int_0^1 \theta(x_i - x_{i-1})\theta(x_i - x_{i+1}) dx_{i-1} dx_i dx_{i+1} \\ &= L \int_0^1 \left[ \int_0^{x_i} \int_0^{x_i} dx_{i-1} dx_{i+1} \right] dx_i = \frac{1}{3}L. \end{aligned} \tag{40}$$

The second central moment  $\mu_2^{1D}$  can be calculated as follows

$$\begin{aligned} \mu_2^{1D} &\equiv \langle M^2 \rangle - \langle M \rangle^2 = \int_0^1 \dots \int_0^1 \left[ \sum_{i=1}^L \sum_{j=1}^L \Delta_i^- \Delta_i^+ \Delta_j^- \Delta_j^+ \{\delta(x_a - x_b)\} \right] dx_1 dx_2 \dots dx_L - \frac{1}{9} L^2 \\ &= L \sum_{j=1}^L \left[ \int_0^1 \dots \int_0^1 \Delta_i^- \Delta_i^+ \Delta_j^- \Delta_j^+ \{\delta(x_a - x_b)\} \right] dx_{i-1} dx_i dx_{i+1} dx_{j-1} dx_j dx_{j+1} - \frac{1}{9} L^2 \\ &= L \left[ \sum_{r=0}^3 a_r^{1D} J_r^{1D} - \frac{1}{9} L \right], \end{aligned} \tag{41}$$

where the notation  $\{\delta(x_a - x_b)\}$  means the following: if some point  $x_a \in \{x_{i-1}, x_i, x_{i+1}\}$  coincides with another point  $x_b \in \{x_{j-1}, x_j, x_{j+1}\}$ , then  $\{\delta(x_a - x_b)\} = 1$  otherwise  $\{\delta(x_a - x_b)\} = 0$  and we sum over all configurations of diagrams shown in Fig. 8a. For example, if in some configuration the points  $x_{i+1}$  and  $x_j$  coincide, then  $\{\delta(x_a - x_b)\} \equiv \delta(x_{i+1} - x_j)$  etc. The value  $J_r^{1D}$  is the integral of the diagram  $r$ ,  $a_r^{1D}$  is the “weight” of the corresponding diagram (i.e. the number of identical diagrams). The graphic representation of integrals in Eq. (41) is given in Fig. 8a. We consider the system of length  $L$  with periodic boundary conditions. Instead of summing over  $L$  possible values of  $i$  we fix some arbitrary value  $x_i$  and perform averaging over all possible positions of  $x_j$ . That gives us  $L$  in front of the sum in (41). The integral in (41) depends on  $j - i$  only. We enumerate all possible values of the integral by the index  $r$ , and compute the weight  $a_r^{1D}$  of each integral  $J_r^{1D}$  in the sum for  $j = 1, 2, \dots, L$ .

The total number of diagrams is normalized:  $\sum_{r=0}^3 a_r^{1D} = L$ . The computed values of  $J_r^{1D}$  and of  $a_r^{1D}$  are collected in the Table 1. All such configurations are generated by shifting the point  $x_j$  with respect to  $x_i$  as shown in Fig. 8a,b.

If the shortest distance between  $x_i$  and  $x_j$  is larger than 2 (respecting the periodic boundary conditions), then the integrals over  $\Delta_i^- \Delta_i^+$  and  $\Delta_j^- \Delta_j^+$  decouple and give  $J_1^{1D} = [P(\uparrow\downarrow)]^2 = \frac{1}{3} \times \frac{1}{3} = \frac{1}{9}$ . The contribution of these integrals cancels by subtracting  $\frac{1}{9}$ . The number of such integrals is  $a_1^{1D} = L - 5$ . The total number of all other configurations is finite and does not depend on  $L$ , so the second central moment is proportional to  $L$  but no to  $L^2$ . Substituting the values from

**Table 1. Values of diagrams  $J_r^{1D}$  and of the corresponding weights  $a_r^{1D}$  for computing  $\mu_2^{1D}$ .**

$r$	0	1	2	3
$J_r^{1D}$	0	$\frac{1}{9}$	$\frac{2}{15}$	$\frac{1}{3}$
$a_r^{1D}$	2	$L - 5$	2	1

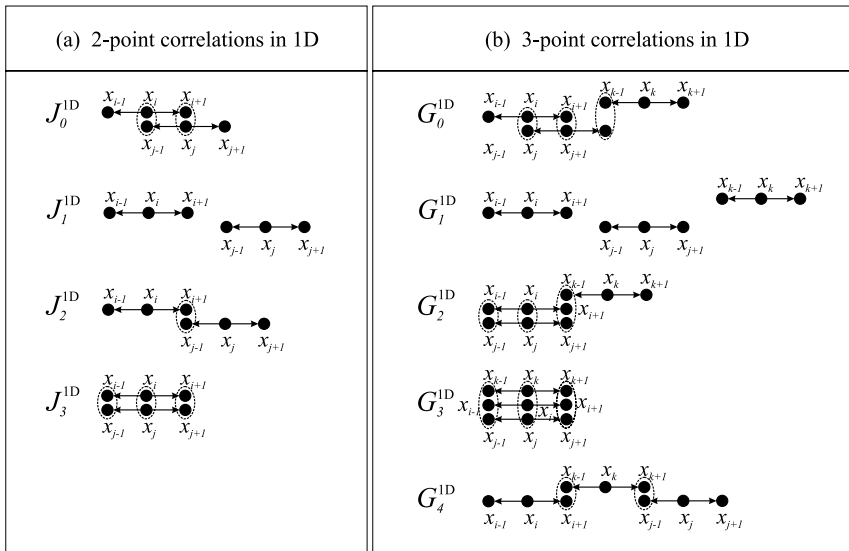


**Fig. 8.** Basic diagrams and corresponding integrals: a)  $J_r^{1D}$  for the computation of  $\mu_2^{1D}$ ; b)  $G_r^{1D}$  for the computation of  $\mu_3^{1D}$ .

the Table 1 into (41), we arrive at the following expression for the second central moment  $\mu_2^{1D}$

$$\mu_2^{1D} = L \left[ \sum_{r=0}^3 a_r^{1D} J_r^{1D} - \frac{1}{9} L \right] = \frac{2}{45} L. \tag{42}$$

To calculate the third central moment  $\mu_3^{1D}$ ,

$$\mu_3^{1D} = \langle (M - \langle M \rangle)^3 \rangle = \langle M^3 \rangle - \langle M \rangle^3 - 3\langle M \rangle (\langle M^2 \rangle - \langle M \rangle^2), \tag{43}$$

we proceed exactly along the same lines as above. The averaged third power of  $M$  is

$$\langle M^3 \rangle = \int_0^1 \dots \int_0^1 \left[ \sum_{i=1}^L \sum_{j=1}^L \sum_{k=1}^L \Delta_i^- \Delta_i^+ \Delta_j^- \Delta_j^+ \Delta_k^- \Delta_k^+ \{ \delta(x_a - x_b) \} \right] dx_1 dx_2 \dots dx_L. \tag{44}$$

This quantity depends only on integrals over three groups of points  $x_{i-1}, x_i, x_{i+1}, x_{j-1}, x_j, x_{j+1}$  and  $x_{k-1}, x_k, x_{k+1}$  and their mutual arrangement. To proceed, we fix some position of  $x_i$  (as it has been done for  $\mu_2^{1D}$ ) and consider the positions of  $x_j$  and  $x_k$  with respect to it. Using the diagrammatic approach we compute integrals  $G_r$  in (44) for each three-point configuration. The corresponding diagrams  $G_r^{1D}$  for  $r = 0, \dots, 4$  are shown in Fig. 8b. We encounter the following possibilities:

(i) The integral (44) contains terms like  $G_0^{1D} = \int \int \theta(x_i - x_j) \theta(x_j - x_i) dx_i dx_j = 0$ ;

(ii) All three points  $x_i, x_j, x_k$  are separate. In such a situation the integrations over three groups of points are independent, giving for each group  $\frac{1}{3}$  according to (40). So, we have  $G_1^{1D} = [P(\uparrow\downarrow)]^3 = \frac{1}{27}$ . All terms of such a type in (43) cancel;

(iii) Two groups have the common points and the third group is separated from them. In this case the separated integration over the third group of points gives  $\langle M \rangle$ . The integration over the rest pair of groups gives just the same result as the contribution to the second central moment. The factor 3 in front of  $(\langle M^2 \rangle - \langle M \rangle^2)$  corresponds to three different ways  $(ij + k, ik + j, jk + i)$  to ascribe the indices to these points. Thus, the contributions from the three-points configurations of such a type and contribution of two-point configurations for  $\langle M^2 \rangle$  in (43) cancel;

(iv) At least two pairs of groups have common points. Such configurations give a non-zero contribution. Integrals for such groups  $G_r^{1D}$  and corresponding weights  $c_r^{1D}$  are summarized in the Table II where  $G_r = J_r$  for  $r = 0, 2, 3$ .

We can split nontrivial ( $r \neq 1$ ) three-point configuration ( $c_r^{1D}$ ) into the two-point configuration by deleting of the one-point group in three different ways. Thus,  $3 \sum_{\substack{r=0 \\ r \neq 1}}^4 c_r^{1D} = \sum_{q=0}^3 b_q^{1D} = 111$ , where  $b_q^{1D}$  is the number of the two-point configurations of type  $q$  obtained as a result of splitting of all possible three-points configurations. The two-point configurations  $b_r^{1D}$  are enumerated in the Table II. The contribution of the two-point configurations are not compensated by an appropriate term from the three-points configurations, so we have to take it into account manually. So, substituting expansion of (44) into (43), we obtain

$$\begin{aligned} \mu_3^{2D} &= \langle M^3 \rangle - \langle M \rangle^3 - 3\langle M \rangle (\langle M^2 \rangle - \langle M \rangle^2) \\ &= L \left[ \sum_{r=0}^4 \left( c_r G_r^{1D} - \frac{1}{27} L \right) - \frac{1}{3} \sum_{q=0}^3 b_q \left( J_q^{1D} - \frac{1}{9} \right) \right] \quad (45) \\ &= -\frac{2}{945} L \simeq -0.0021164L. \end{aligned}$$

**Table II. Values of integrals  $G_r^{1D}$  and of the weights  $c_r^{1D}$  (left) for the three-point configurations and values of integrals  $J_r^{1D}$  and weights  $b_r^{1D}$  (right) for computing  $\mu_3^{1D}$ .**

$r$	0	1	2	3	4
$G_r^{1D}$	0	$\frac{1}{27}$	$\frac{2}{15}$	$\frac{1}{3}$	$\frac{17}{315}$
$c_r^{1D}$	24	$L - 37$	6	1	6
$J_r^{1D}$	0	$\frac{1}{9}$	$\frac{2}{15}$	$\frac{1}{3}$	
$b_r^{1D}$	36	18	42	15	



It is worth mentioning that the moments in Eqs. (40), (42) and (45), calculated using the operator technique, coincide with the ones obtained on the basis of exact combinatorial approach (23).

### 5. CONDITIONAL PROBABILITY $p(l)$ OF TWO PEAKS SEPARATED BY DISTANCE $l$

We aim now at evaluating the probability  $p(l)$  of having two peaks separated by a distance  $l$ , under the condition that there are no peaks (i.e. sequences  $\uparrow \downarrow$ ) on the interval between these peaks. According to Ref. 24, this probability is given by

$$p(l) = \int_0^1 dx \sum Q(x), \tag{46}$$

where the sum is taken over all possible peak-avoiding rise-and-descent patterns of length  $l$  between two peaks, while  $Q(x)$  denote the  $Q$ -polynomials corresponding to each given configuration (see the explanations above).

There are several possible peak-avoiding “rise-and-descent“ sequences contributing to such a probability. These sequences are depicted in Fig. 9. The first peak is located at 0 position, the second peak is located at  $l$  position. We have fixed a descent at 1st position (variable  $Y$ ) to keep a peak at the 0s position (variable  $X$ ).

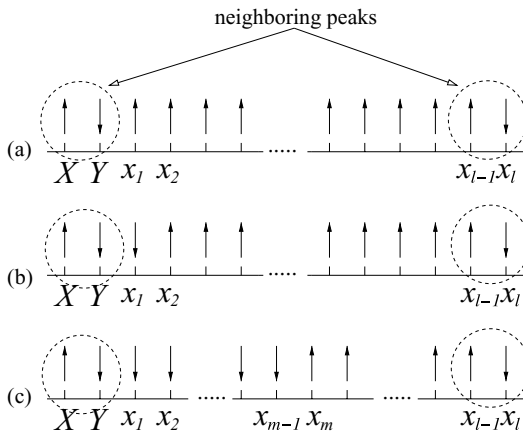


**Fig. 9.** Rise-and-descent patterns contributing to the conditional probability of having two closest peaks at distance  $l$  apart from each other. Configuration (a) has only one descent between two peaks. Configuration (b) has two descents following the first peak, i.e. a “through” at  $x_1$ , and (c) presents a generalization of (b) over configurations having  $m$  descents, ( $m = 1, 2, \dots, l$ ), after the first peak which are followed by  $l - m$  rises, i.e. a “through” at  $x_{m-1}$ ,

Now, the  $Q$ -polynomial associated with the sequence (a) in Fig. 9 has the following form:

$$Q^a(x) = \int_x^1 dX \int_0^X dY \int_Y^1 dx_1 \int_{x_1}^1 dx_2 \dots \int_{x_{l-2}}^1 dx_{l-1} \int_0^{x_{l-1}} dx_l. \quad (47)$$

Performing the integration over  $x_{l+1}$  in the latter expression, we denote the iterated integrals over the variables  $x_k, k = 1, 2, 3 \dots, l$  as

$$M_l(Y) = \int_Y^1 dx_1 \int_{x_1}^1 dx_2 \dots \int_{x_{l-1}}^1 x_l dx_l. \quad (48)$$

Notice now that  $M_l$  obey the following recursion scheme:

$$M_l(Y) = \int_Y^1 M_{l-1}(X) dX, \quad M_0(Y) = Y. \quad (49)$$

Introducing the generating function of the form:

$$M(Y) = \sum_{l=0}^{\infty} M_l(Y)z^l, \quad (50)$$

we readily find that it obeys

$$M(Y) - Y = z \int_Y^1 M(X) dX, \quad (51)$$

and consequently,  $M_l$  are simply the coefficients in the expansion

$$M(Y) = \sum_{l=0}^{\infty} M_l z^l = \frac{1}{z} [1 - (1 - z) \exp(z(1 - x))], \quad (52)$$

which are given explicitly by

$$M_l(Y) = \frac{(1 - Y)^l}{l!} - \frac{(1 - Y)^{l+1}}{(l + 1)!} = \frac{1}{(l + 1)!} (l + Y)(1 - Y)^l. \quad (53)$$

Hence, the  $Q$ -polynomial associated with the configuration (a) in Fig. 9 obeys

$$Q^a(x) = \int_x^1 dX \int_0^X M_{l-1}(Y) dY = \frac{1}{l!} \int_x^1 dX \int_0^X [(1 - Y)^{l-1} (l - 1 + Y)] dY, \quad (54)$$

and the contribution of this very configuration to the probability  $p(l)$  reads:

$$p^a(l) = \frac{1}{l!} \int_0^1 dx \int_x^1 dX \int_0^X [(1 - Y)^{l-1} (l - 1 + Y)] dY. \quad (55)$$

Next, we turn to the contribution coming out of the general configuration (c) in Fig. 9. The  $Q$ -polynomial associated with this configuration of rises and descents for a fixed  $m$  is given by

$$\begin{aligned}
 Q^c(x, m) &= \int_x^1 dX \int_0^X dY \int_0^Y dx_1 \int_0^{x_1} dx_2 \int_0^{x_2} dx_3 \dots \\
 &\quad \int_0^{x_{m-2}} dx_{m-1} \int_{x_{m-1}}^1 dx_m \dots \int_{x_{l-2}}^1 dx_{l-1} \int_0^{x_{l-1}} dx_l \\
 &= \int_x^1 dX \int_0^X dY \int_0^Y dx_1 \int_0^{x_1} dx_2 \int_0^{x_2} dx_3 \dots \\
 &\quad \int_0^{x_{m-2}} dx_{m-1} \int_{x_{m-1}}^1 dx_m \dots \int_{x_{l-2}}^1 dx_{l-1} dx_l \\
 &= \int_x^1 dX \int_0^X dY \int_0^Y dx_1 \int_0^{x_1} dx_2 \int_0^{x_2} dx_3 \dots \\
 &\quad \int_0^{x_{m-2}} M_{l-m}(x_{m-1}) dx_{m-1}. \tag{56}
 \end{aligned}$$

Let us note, that  $Q^a(x) = Q^c(x, m = 1)$ . Consider next a recursion scheme of the form

$$N_m(Y) = z \int_0^Y N_{m-1}(X) dX, \tag{57}$$

where  $N_0(Y)$  is some arbitrary function  $\Phi(Y)$ . Introducing the generating function

$$N(Y) = \sum_{m=0}^{\infty} N_m(Y) z^m, \tag{58}$$

we get that it obeys

$$N(Y) - \Phi(Y) = z \int_0^Y N(X) dX. \tag{59}$$

Solution of the latter equation can be readily obtained by standard means and reads

$$N(Y) = \Phi(0) \exp(zY) + \int_0^Y \frac{d\Phi(X)}{dX} \exp(z(Y - X)) dX. \tag{60}$$

Finally, expanding the rhs of the latter equation in powers of  $z$ , we get that  $N_m(Y)$  are given explicitly by

$$N_m(Y) = \Phi(0) \frac{Y^m}{m!} + \int_0^Y \frac{d\Phi(X)}{dX} \frac{(Y - X)^m}{m!} dX = \int_0^Y \Phi(X) \frac{(Y - X)^{m-1}}{(m - 1)!} dX. \tag{61}$$

Now, we notice that, as a matter of fact, the multiple integral over the variables  $Y$  and  $x_k, k = 1, 2, \dots, m - 1$  on the rhs of Eq. (56) becomes just the function  $N_m(Y)$ , if one takes  $\Phi(Y) = M_{l-m}(Y)$ . This implies that

$$\begin{aligned} & \int_0^X dY \int_0^Y dx_1 \int_0^{x_1} dx_2 \dots \int_0^{x_{m-2}} M_{l-m}(x_{m-1}) dx_{m-1} \\ &= \int_0^X \frac{(X - Y)^{m-1} (1 - Y)^{l-m} (l - m + Y)}{(m - 1)! (l - m + 1)!} dY. \end{aligned} \tag{62}$$

Substituting  $m = 1$  we obtain here  $\int_0^X M_{l-1} dY$ . Consequently, we find that the desired probability obeys

$$p(l) = \int_0^1 dx \int_x^1 dX \int_0^X \left[ \sum_{m=1}^{l-1} \frac{(X - Y)^{m-1} (1 - Y)^{l-m} (l - m + Y)}{(m - 1)! (l - m + 1)!} \right] dY. \tag{63}$$

Let us introduce the generating function  $F(z) = \sum_{l=2}^{\infty} z^l p(l)$ . We can represent the sum

$$\sum_{l=2}^{\infty} \sum_{m=1}^{l-1} z^l f(l, m) = \sum_{m=1}^{\infty} \sum_{k=1}^{\infty} z^{k+m} f(k + m, m), \tag{64}$$

where  $k = l - m$ . Using

$$\sum_{m=1}^{\infty} z^m \frac{(X - Y)^{m-1}}{(m - 1)!} = ze^{z(X-Y)}, \tag{65}$$

and

$$\sum_{k=1}^{\infty} z^k (k + Y) \frac{(1 - Y)^k}{(k + 1)!} = e^{z(1-Y)} \left( 1 - \frac{1}{z} \right) + \frac{1}{z} - Y, \tag{66}$$

we obtain

$$\begin{aligned} F(z) &= \sum_{l=2}^{\infty} z^l \left( \int_0^1 dx \int_x^1 dX \int_0^X \left[ \sum_{m=1}^{l-1} \frac{(X - Y)^{m-1} (1 - Y)^{l-m} (l - m + Y)}{(m - 1)! (l - m + 1)!} \right] dY \right) \\ &= \int_0^1 dx \int_x^1 dX \int_0^X \left[ \sum_{m=1}^{\infty} \sum_{k=1}^{\infty} \left( z^m \frac{(X - Y)^{m-1}}{(m - 1)!} \right) \left( z^k \frac{(1 - Y)^k (k + Y)}{(k + 1)!} \right) \right] dY \\ &= \int_0^1 dx \int_x^1 dX \int_0^X \left[ ze^{z(X-Y)} \left( e^{z(1-Y)} \left( 1 - \frac{1}{z} \right) - Y + \frac{1}{z} \right) \right] dY \\ &= \frac{(z - 1)^2}{2z^3} e^{2z} + \left( \frac{1}{3} + \frac{1}{2z} - \frac{1}{2z^3} \right). \end{aligned} \tag{67}$$

Hence, the generating function is given by

$$F(z) = \frac{2}{15}z^2 + \frac{1}{9}z^3 + \frac{2}{35}z^4 + \frac{1}{45}z^5 + \frac{4}{567}z^6 + \dots \tag{68}$$

Note that the numerical values  $\frac{2}{15}$  (for  $l = 2$ ) and  $\frac{1}{9}$  (for  $l = 3$ ) correspond to the values obtained in Ref. 24. In general, we get the following explicit expression

$$p(l) = \frac{1}{2} \left( \frac{2^{l+1}}{(l+1)!} - 2 \frac{2^{l+2}}{(l+2)!} + \frac{2^{l+3}}{(l+3)!} \right) = 2^l \frac{(l-1)(l+2)}{(l+3)!}, \tag{69}$$

which defines the probability  $p(l)$  of finding two peaks separated by the distance  $l$  with no peaks between these two points for arbitrary  $l$ . The function  $p(l)$  is depicted in Fig. 10.

Note also that  $p(l)$  in Eq. (69) coincides with the distribution function of the distance between two “weak” bonds obtained by Derrida and Gardner.<sup>(27)</sup>

### 6. PROBABILITY DISTRIBUTION FUNCTION $P(M,L)$ IN 2D

In this last section we are going to study the statistics of peaks in a two-dimensional BD landscape  $h(i, j, n)$  by converting this problem to the analysis of the distribution of peaks in the associated permutation matrix.

It is convenient to represent the two-dimensional base  $(i, j)$ ,  $(i, -j = 1, 2, 3, \dots, m, m \times m = L)$  as a one-dimensional set with long-ranged correlations. Namely, reading the lattice  $(i, j)$  from the left to the right in the line and line-by-line from top-to-bottom, exactly as an electron beam does to highlight the image on the TV screen, we can rewrite equations (3) and (4) renaming  $h(i, j, n)$  as:  $h(i, j, n) \equiv h(k, n)$ , where  $k = 1, 2, 3, \dots, L$ . Hence,  $h(i - 1, j, n) \equiv h(k - 1, n)$ ;  $h(i + 1, j, n) \equiv h(k + 1, n)$ ;  $h(i, j - 1, n) \equiv h(k - m, n)$ ;  $h(i, j + 1, n) \equiv h(k + m, n)$ , where  $1 \leq k \leq L$ .

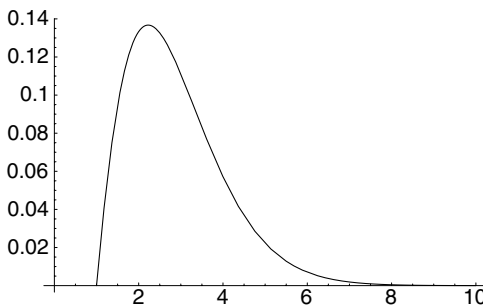


**Fig. 10.** Probability of having two peaks being at distance  $l$  apart of each other with no peaks inbetween. It has a maximum at  $l = 2$ .

Given Eq. (3), we can describe the growth of a two-dimensional BD landscape over the base  $m \times m$  as a stationary “updating dynamics” in the  $L \times L$  permutation matrix with the uniform distribution on updating events. The uniform “updating dynamics” on permutations generates the PDF of peaks identical to the PDF of peaks computed over the ensemble of all  $L!$  equally weighted permutations (compare to the one-dimensional case). Thus, repeating the arguments of the previous section, we can construct an analogue a two-dimensional PGRW for permutation matrix with finite-length correlations.

The most significant and the only difference between one-and two-dimensional models is in the definition of a “peak.” In 1D case, a peak appears at the position  $k$  of the permutation matrix if the corresponding permutation  $\pi_k$  is larger then the nearest neighboring permutations  $\pi_{k-1}$  and  $\pi_{k+1}$ . In 2D case,  $k$  is a peak if and only if  $\pi_k$  is larger than  $\pi_{k-1}$ ,  $\pi_{k+1}$ ,  $\pi_{k-m}$  and  $\pi_{k+m}$  simultaneously. In the next subsection we generalize the operator formalism over the 2D case and calculate the PDF of peaks for the uniform BD process in two dimensions.

### 6.1. Central Moments of the Probability Distribution Function in 2D

To obtain the limiting ( $L \rightarrow \infty$ ) Probability Distribution Function  $P(M, L)$  of having exactly  $M$  peaks on a two-dimensional square base  $L = m \times m$ , we calculate the first three central moments of the distribution function and then construct the corresponding Edgeworth series (cumulant expansion).<sup>(25)</sup> This enables us: a) to show that in the limit  $L \rightarrow \infty$  the function  $P(M, L)$  converges to the Gaussian distribution, and b) to present an explicit expression for  $P(M, L)$  in this limit.

The total number of points for 2D system is  $L = m^2$ . Applying to the 2D case the same arguments as in 1D case, we define

$$\begin{aligned}
 \Delta_{i,j}^\uparrow &= \theta(x_{i,j} - x_{i-1,j}) \text{ for the “northern” neighbor} \\
 \Delta_{i,j}^\rightarrow &= \theta(x_{i,j} - x_{i,j+1}) \text{ for the “western” neighbor} \\
 \Delta_{i,j}^\downarrow &= \theta(x_{i,j} - x_{i+1,j}) \text{ for the “southern” neighbor} \\
 \Delta_{i,j}^\leftarrow &= \theta(x_{i,j} - x_{i,j-1}) \text{ for the “eastern” neighbor,}
 \end{aligned}
 \tag{70}$$

(compare (70) to (38)).

Using the operator formalism we obtain for the first central moment

$$\begin{aligned}
 \mu_1^{2D} &= \int_0^1 \dots \int_0^1 \left[ \sum_{i=1}^m \sum_{j=1}^m \Delta_{i,j}^\uparrow \Delta_{i,j}^\rightarrow \Delta_{i,j}^\downarrow \Delta_{i,j}^\leftarrow \right] dx_{1,1} dx_{1,2} \dots dx_{m,m-1} dx_{m,m} \\
 &= L \int_0^1 \dots \int_0^1 \Delta_{i,j}^\uparrow \Delta_{i,j}^\rightarrow \Delta_{i,j}^\downarrow \Delta_{i,j}^\leftarrow dx_{i-1,j} dx_{i,j+1} dx_{i+1,j} dx_{i,j-1} dx_{i,j} = \frac{1}{5} L.
 \end{aligned}
 \tag{71}$$

As in 1D, all terms in (71) are identical and independent.

**Table III. Values of integrals  $J_r^{2D}$  and of the weights  $a_r^{2D}$  for computing  $\mu_2^{2D}$ .**

$r$	0	1	2	3	4
$J_r^{2D}$	0	$\frac{1}{25}$	$\frac{2}{45}$	$\frac{1}{20}$	$\frac{1}{5}$
$a_r^{2D}$	4	$N - 13$	4	4	1

2. The same method is used for computing the second central moment. We define  $d\mathbf{x}_{i,j} = dx_{i-1,j} dx_{i,j+1} dx_{i+1,j} dx_{i,j-1} dx_{i,j}$  for integration over the point  $x_{i,j}$  and its 4 neighbors to make the expressions more compact. Instead of summing over  $i, j$ , we fix the position of the first point  $x_{i,j}$  and perform the summation over all possible positions of  $x_{k,l}$  with respect to  $x_{i,j}$ . Then we enumerate all different integrals  $J_r^{2D}$  and compute the corresponding weights  $a_r^{2D}$ . The configurations which contribute to  $J_r^{2D}$  are shown in Fig. 11a,b. As in 1D case, the  $\delta(x_{a,b} - x_{c,d})$  cut off the diagrams with coinciding points (see the explanation after (41)).

The values of integrals  $J_r^{2D}$  and their weights  $a_r^{2D}$  are collected in Table III.

The total number of integrals is  $\sum_{r=0}^4 a_r^{2D} = L = m^2$ . The contribution from the integral  $J_1^{2D}$  is exactly canceled by the term  $-\frac{1}{25}$  coming from two independent points:

$$\begin{aligned}
 \mu_2^{2D} &= \int_0^1 \dots \int_0^1 \left[ \sum_{i=1}^m \sum_{j=1}^m \sum_{k=1}^m \sum_{l=1}^m \Delta_{i,j}^\uparrow \Delta_{i,j}^\rightarrow \Delta_{i,j}^\downarrow \Delta_{i,j}^\leftarrow \Delta_{k,l}^\uparrow \Delta_{k,l}^\rightarrow \Delta_{k,l}^\downarrow \Delta_{k,l}^\leftarrow \{ \delta(x_{a,b} - x_{c,d}) \} \right] \\
 &\quad \times dx_{1,1} dx_{2,1} \dots dx_{m,m} - \frac{1}{25} L^2 \\
 &= L \sum_{k=1}^m \sum_{l=1}^m \left[ \int_0^1 \dots \int_0^1 \Delta_{i,j}^\uparrow \Delta_{i,j}^\rightarrow \Delta_{i,j}^\downarrow \Delta_{i,j}^\leftarrow \Delta_{k,l}^\uparrow \Delta_{k,l}^\rightarrow \Delta_{k,l}^\downarrow \Delta_{k,l}^\leftarrow \{ \delta(x_{a,b} - x_{c,d}) \} d\mathbf{x}_{i,j} \right] \\
 &\quad \times d\mathbf{x}_{k,l} - \frac{1}{25} L^2 \\
 &= L \sum_{r=0}^4 \left[ a_r^{2D} J_r^{2D} - \frac{1}{25} L \right] = \frac{13}{225} L. \tag{72}
 \end{aligned}$$

3. For computation of the third moment in 2D we use again the same method as in 1D. Namely, we fix the first point  $x_{i,j}$  and enumerate all possible configurations of three points. Different types of three-points configurations are depicted in Fig. 11b). Other configurations with the same contribution  $G_r^{2D}$  and the same topologies but slightly different conformations are not shown in the figure. The integrals  $G_r^{2D}$  and  $J_r^{2D}$  have the same values for  $r = 0, 2, 3, 4$ . In the configuration

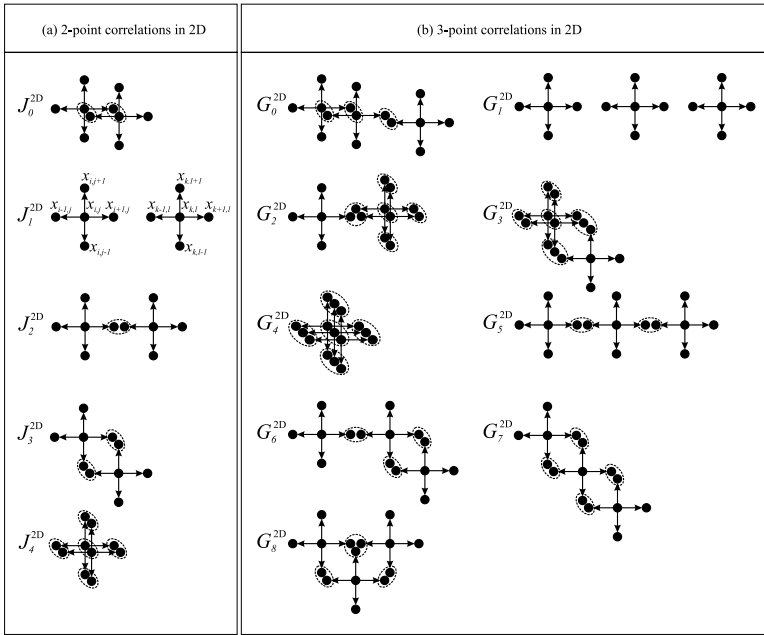


**Fig. 11.** Basic diagrams and corresponding integrals: (a)  $J_r^{2D}$  for the computation of  $\mu_2^{2D}$ ; (b)  $G_r^{2D}$  for the computation of  $\mu_3^{2D}$ .

$G_4^{2D}$  all three points coincide, so  $G_4^{2D} = \frac{1}{5}$ . The most general form of the integral  $G_r^{2D}$  is as follows

$$G_r^{2D} = \int_0^1 \dots \int_0^1 \Delta_{i,j}^\uparrow \Delta_{i,j}^\rightarrow \Delta_{i,j}^\downarrow \Delta_{i,j}^\leftarrow \Delta_{k,l}^\uparrow \Delta_{k,l}^\rightarrow \Delta_{k,l}^\downarrow \Delta_{k,l}^\leftarrow \Delta_{m,n}^\uparrow \Delta_{m,n}^\rightarrow \Delta_{m,n}^\downarrow \Delta_{m,n}^\leftarrow \times \{\delta(x_{a,b} - x_{c,d})\} d\mathbf{x}_{i,j} d\mathbf{x}_{k,l} d\mathbf{x}_{m,n}, \tag{73}$$

where  $d\mathbf{x}_{i,j} = dx_{i-1,j} dx_{i,j-1} dx_{i+1,j} dx_{i,j+1} dx_{i,j}$  and the  $\delta$ -functions in (73) cut off the coinciding points. For example, if in some configuration the points  $x_{i,j+1}$  and  $x_{k,l-1}$  coincide, then we include the function  $\delta(x_{k,l-1} - x_{i,j+1})$  etc.

It is possible to simplify integrals of such a type by changing the limits of integration. For example,  $\int_0^1 \int_0^1 \Delta_{i,j}^\uparrow dx_{i,j} dx_{i-1,j} = \int_0^1 x_{i,j} dx_{i,j}$ . In such a way the integral  $G_5^{2D}$  can be expressed as follows:

$$G_5^{2D} = \int_0^1 dx_{i,j} \left[ x_{i,j}^3 \int_0^{x_{i,j}} dx_{i,j+1} \left[ \int_{x_{i,j+1}}^1 dx_{i,j+2} \left[ x_{i,j+2}^2 \int_0^{x_{i,j+2}} dx_{i,j+3} \right. \right. \right. \left. \left. \left. \times \left[ \int_{x_{i,j+3}}^1 x_{i,j+4}^3 dx_{i,j+4} \right] \right] \right] \right] = \frac{29}{2925}. \tag{74}$$



**Table IV. Three-point configurations for computing  $\mu_3^{2D}$ : integrals  $G_r^{2D}$  and weights  $c_r^{2D}$  (left) and integrals  $J_r^{2D}$  and weights  $b_r^{2D}$  (right).**

$r$	0	1	2	3	4	5	6	7	8
$G_r^{2D}$	0	$\frac{1}{125}$	$\frac{2}{45}$	$\frac{1}{20}$	$\frac{1}{5}$	$\frac{29}{2925}$	$\frac{121}{10800}$	$\frac{7}{550}$	$\frac{13}{990}$
$c_r^{2D}$	168	$N - 313$	12	12	1	36	48	12	24
$J_r^{2D}$	0	$\frac{1}{25}$	$\frac{2}{45}$	$\frac{1}{20}$	$\frac{1}{5}$				
$b_r^{2D}$	216	216	252	216	39				

The values of integrals  $G_0^{2D} - G_8^{2D}$  are collected in the Table IV.

The symmetry of configurations defines the weights  $c_r$ . For example, the diagram of the integral  $G_5^{2D}$  in Fig. 11b has two orientations along vertical and horizontal lines. Thus the total weight of the integral  $G_5^{2D}$  is  $c_5^{2D} = 36$ .

The values of  $c_r$  are given in the Table IV. Totally there are  $\sum_{\substack{r=0 \\ r \neq 1}}^8 c_r^{2D} = 313$  different nontrivial configurations. We can split each of the nontrivial three-points configuration as it has been done in 1D case. There are three ways to do it. Values of  $b_r$  of the corresponding two-point configurations are shown in the Table IV with the total number  $\sum_{r=0}^4 b_r^{2D} = 939$  of such configurations. Now it is possible to compute the third moment

$$\begin{aligned} \mu_3^{2D} &= L \left[ \sum_{r=0}^8 \left( c_r^{2D} G_r^{2D} - \frac{1}{125} L \right) - \frac{1}{5} \sum_{r=0}^4 b_r^{2D} \left( J_r^{2D} - \frac{1}{25} \right) \right] \\ &= \frac{512}{32175} L \simeq 0.015913L. \end{aligned} \tag{75}$$

### 6.2. The Distribution Function $P(M, L)$ in the Limit $L \rightarrow \infty$

The cumulants  $\kappa_i^{2D}$  of  $P(M, L)$  are equal to the central moments,  $\mu_i^{2D}$ , ( $i = 1, 2, 3$ ), where

$$\begin{cases} \mu_2^{2D} = \sigma^2 = \frac{13}{225} L \\ \mu_3^{2D} = \frac{512}{32175} L \end{cases} \tag{76}$$

Introducing the normalized deviation,  $x = M - \mu_1^{2D} / \sigma$ , we can write the normalized probability distribution  $p(x, L) = P(\mu_1^{2D} + x\sigma, L)$  in a form of the Edgeworth series (cumulant expansion)<sup>(25)</sup>

$$p(x, L) \simeq g(x) \left( 1 + \frac{1}{\sqrt{L}} f(x) + o\left(\frac{1}{\sqrt{L}}\right) \right), \tag{77}$$

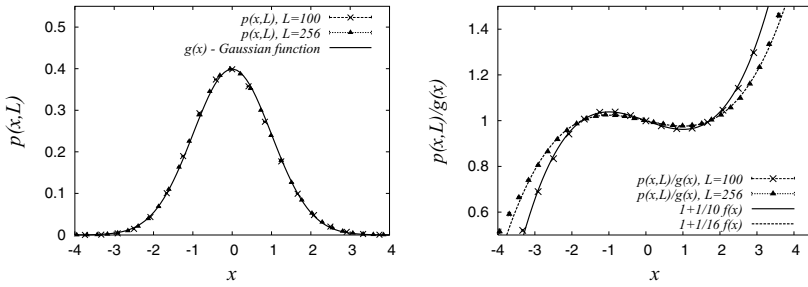


**Fig. 12.** (a) Results of numerical simulation of  $p(x, L)$  for  $L = 100, 256$ : (a) comparison of  $p(x, L)$  with the Gaussian function  $g(x)$ ; (b) comparison of the function  $p(x, L)/g(x)$  with  $1 + \frac{1}{L} f(x)$ .

where  $g(x)$  is the Gaussian function  $g(x) = 1/\sqrt{2\pi} e^{-x^2/2}$ , and  $f(x)$  is defined by  $\mu_2^{2D}$  and  $\mu_3^{2D}$  (see Ref. 25 for details)

$$f(x) = \sqrt{L} \frac{\kappa_3^{2D}}{(\kappa_2^{2D})^{3/2}} \frac{1}{6} (x^3 - 3x) \tag{78}$$

Substituting (76) in (78), we get

$$f(x) = \frac{512}{32175} \left( \frac{225}{13} \right)^{3/2} \frac{1}{6} (x^3 - 3x). \tag{79}$$

Let us emphasize that  $f(x)$  does not depend on  $L$ , as one may readily check by substituting exact results obtained for the cumulants to Eq. (78). To verify the expression in (79), we have performed the numerical simulations for the discrete 2D permutation-generated model with the periodic boundary conditions and have computed the distribution function  $p(x, L)$  numerically. In Fig. 12a we present the data of the numerical simulations for  $p(x, L)$  and compare it against the Gaussian function  $g(x)$  for system sizes  $L = 100$  and  $256$ . Furthermore, in Fig. 12b we plot the ratio  $\frac{p(x, L)}{g(x)}$  as the function of  $x$ , which shows that the deviation of the numerically computed function  $p(x, L)$  from the Gaussian function  $g(x)$  is actually very small.

One clearly sees that for  $L \rightarrow \infty$  the normalized probability distribution function  $p(x, L)$  converges to the Gaussian function  $g(x)$ .

## 7. CONCLUSION

To conclude, we have studied the probability distribution function  $P(M, L)$  of the number of local peaks in one- and two-dimensional surfaces obtained in a standard model of next-nearest-neighbor ballistic deposition process. Our analysis was based on two central results:

- (i) A proof, presented in this paper, of the fact that a ballistic deposition process in the steady state can be formulated exactly in terms of “rise-and-descent”

patterns in the ensemble of random permutation matrices, which made it possible to interpret the BD model in terms of permutations of the set  $1, 2, 3, \dots, L$ , where  $L$  is the number of lattice sites and the numbers drawn at random from this set determine local heights of the surface.

(ii) An observation made in Ref. 24, that the “rise-and-descent” patterns can be treated efficiently using a recently proposed algorithm of a Permutation Generated Random Walk.

In one-dimensional case we have found a closed-form expression (28) for the generating series  $W(s, L) = L! \sum_{M=0}^{\infty} s^{M+1} P(M, L)$  of the distribution function  $P(M, L)$  of peaks in a bounding box of size  $L$ . Inverting this expression, we got an exact and asymptotic forms of  $P(M, L)$ .

Besides, in one-dimension we calculated the probability  $p(l)$  of having two peaks separated by a distance  $l$ , under the condition that there are no peaks in the interval between these two peaks. The function  $p(l)$  is given by expression (69).

For two-dimensional case, we reformulated the BD process in terms of an “updating dynamics” on permutations with certain finite-range correlations. Using this approach, we extended the operator formalism of Ref. 24, to such correlated permutations and evaluated three first central moments of the PDF. Then, we have obtained  $P(M, L)$  in the asymptotic limit  $L \rightarrow \infty$  using expansions in the Edgeworth series<sup>(25)</sup>—see (77)–(79). We have shown that in 2D the PDF also converges to a Gaussian function as  $L \rightarrow \infty$ .

## APPENDIX A

Let us exploit the relation between the generating function of peaks,

$$W(s, L) = L! \sum_{M=0}^{\infty} s^{M+1} P(M, L)$$

and *Poly-log* function (see Ref. 21, for details):

$$\frac{1}{2} \frac{(1+t)^{L+1}}{(1-t)^{L+1}} W\left(\frac{4t}{(1+t)^2}, L\right) = \sum_{m=1}^{\infty} (2m)^{L+1} t^m \tag{A.1}$$

Introducing  $s = \frac{4t}{(1+t)^2}$ , rewrite (A.1) taking into account that  $t = \frac{(1-\sqrt{1-s})^2}{s}$ :

$$W(s, L) = 2(1-s)^{(L+1)/2} \sum_{m=1}^{\infty} (2m)^{L+1} \left[ \frac{(1-\sqrt{1-s})^2}{s} \right]^m \tag{A.2}$$

Use now the expansions

$$\begin{aligned}
 (1 - s)^{(L+1)/2} &= 2\Gamma\left(\frac{L+3}{2}\right) \sum_{j=0}^{\infty} \frac{(-1)^j}{j! \Gamma\left(\frac{L+3}{2} - j\right)} s^j; \\
 (1 - \sqrt{1-s})^q &= q \left(\frac{s}{2}\right)^q \sum_{j=0}^{\infty} \frac{\Gamma(q+2j)}{j! \Gamma(q+j+1)} \left(\frac{s}{4}\right)^j
 \end{aligned}
 \tag{A.3}$$

Define now

$$\begin{aligned}
 a(i, L) &= \frac{(-1)^i}{i! \Gamma\left(\frac{L+3}{2} - i\right)} \\
 b(m, L) &= (2m)^{L+1} 2^{-2m} \\
 c(m, L) &= \frac{\Gamma(2m+2j)}{j! \Gamma(2m+j+1)} 2^{-2j}
 \end{aligned}
 \tag{A.4}$$

and rewrite  $W(s, L)$  in (A.2) as follows

$$W(s, L) = 2\Gamma\left(\frac{L+3}{2}\right) \sum_{i=0}^{\infty} a(i, L) s^i \sum_{m=1}^{\infty} b(m, L) s^m \sum_{j=0}^{\infty} c(m, j) s^j
 \tag{A.5}$$

After resummation of (A.5) we arrive at the following expression:

$$W(s, L) = 2\Gamma\left(\frac{L+3}{2}\right) \sum_{M=0}^{\infty} \left[ \sum_{l=1}^M a(M-l, L) \sum_{m=1}^l b(m, L) c(m, l-m) \right] s^M
 \tag{A.6}$$

Hence, by definition of the generating series, we get

$$\begin{aligned}
 P(M, L) &= \frac{2\Gamma\left(\frac{L+3}{2}\right)}{L!} \sum_{l=1}^M \frac{(-1)^{M-l}}{(M-l)! \Gamma\left(\frac{L+3}{2} - M + l\right)} \sum_{m=1}^l \frac{(2m)^{L+1}}{(l-m)! \Gamma(m+l+1)} \\
 &= \frac{2^{L+2}}{L!} \sum_{l=1}^M (-1)^{M-l} \binom{\frac{L+1}{2}}{M-l} \sum_{m=1}^l \frac{m^{L+1}}{(l-m)!(l+m)!}
 \end{aligned}
 \tag{A.7}$$

what gives the desired final expression for PDF  $P(M, L)$  in one dimension.

### ACKNOWLEDGMENTS

The authors are grateful to R.Voituriez for helpful discussions. We are also indebted to B.Derrida for discussions and remarks, as well as for communicating us his unpublished results. F.H. and S.N. wish to thank the members of the laboratory J.-V.Poncelet (Independent University, Moscow), where this work was started, for valuable comments and warm hospitality. G.O. acknowledges financial support from the Alexander von Humboldt Foundation via the Bessel Research Award. The work is partially supported by the grant ACI-NIM-2004-243 ‘‘Nouvelles Interfaces des Mathématiques’’ (France).

## REFERENCES

1. M. Kardar, G. Parisi and Y.-C. Zhang, *Phys. Rev. Lett.* **56**:889 (1986).
2. S. F. Edwards and D. R. Wilkinson, *Proc. Roy. Soc. London A* **381**:17 (1982).
3. S. N. Majumdar and A. Comtet, *Phys. Rev. Lett.* **92**:225501 (2004).
4. M. A. Herman and H. Sitter, *Molecular beam epitaxy: Fundamentals and current*, (Springer: Berlin, 1996).
5. P. Meakin, *Fractals, Scaling, and Growth Far From Equilibrium*, (Cambridge University Press: Cambridge, 1998).
6. M. Prähofer and H. Spohn, *Phys. Rev. Lett.* **84**:4882 (2000).
7. J. Baik and E. M. Rains, *J. Stat. Phys.* **100**:523 (2000).
8. K. Johansson, *Comm. Math. Phys.* **242**:277 (2003).
9. C. A. Tracy and H. Widom, *Commun. Math. Phys.* **159**:151 (1994).
10. B. B. Mandelbrot, *The fractal Geometry of nature*. Freeman, New York, 1982.
11. P. Meakin, P. Ramanlal, L. M. Sander and R. C. Ball, *Phys. Rev. A* **34**:5091 (1986).
12. J. Krug and P. Meakin, *Phys. Rev. A* **40**:2064 (1989).
13. D. Blomker, S. Maier-Paape and T. Wanner, *Interfaces and Free Boundaries* **3**:465 (2001).
14. G. Costanza, *Phys. Rev. E* **55**:6501 (1997).
15. F. D. A. Aarao Reis, *Phys. Rev. E* **63**:056116 (2001).
16. E. Katzav and M. Schwartz, *Phys. Rev. E* **70**:061608 (2004).
17. B. Derrida, private communication.
18. S. Nechaev and R. Bikbov, *Phys. Rev. Lett.* **87**:150602 (2001).
19. Z. Toroczkai, G. Korniss, S. Das Sarma and R. K. P. Zia, *Phys. Rev. E* **62**:276 (2000).
20. J. Desbois, *J. Phys. A: Math. Gen.* **34**:1953 (2001).
21. J. R. Stembridge, *Trans. Am. Math. Soc.* **349**:763 (1997).
22. N. Bergeron, F. Hivert and J. -Y. Thibon, *J. Combinatorial Theory A* **117**(1): (2004).
23. L. J. Billera, S. K. Hsiao and S. Van Willigenburg, *Adv. Math.* **176**:248 (2003).
24. G. Oshanin and R. Voituriez, *J. Phys. A: Math. Gen.* **37**:6221 (2004).
25. H. Cramér, *Mathematical methods of Statistics*, (Princeton University Press: Princeton, 1957).
26. Only the particle of the roof  $\mathcal{T}$  can be removed from the pile without disturbing the rest of the heap—as in the *micado* game.
27. B. Derrida and E. Gardner, *J. Phys. (Paris)* **47**:959 (1986).
28. J. M. Hammersley, *Proc. 6th Berkeley Symp. Math. Statist. and Probability, Vol. 1.* (Berkeley, CA: University of California Press, 1972), p. 345.
29. D. Aldous and P. Diaconis, *Probab. Theory Relat. Fields* **103**:199 (1995).